Office de la propriété intellectuelle du Canada
Un organisme d'Industrie Canada

Canadian Intellectual Property Office
An Agency of Industry Canada

PC CA 00/00469
23 MAY 2000 (23.05.00)

CA00/00469

Bureau canadien des brevets
Certification

Canadian Patent Office
Certification

4

La présente atteste que les documents ci-joints, dont la liste figure ci-dessous, sont des copies authentiques des documents déposés au Bureau des brevets.

This is to certify that the documents attached hereto and identified below are true copies of the documents on file in the Patent Office.

Specification and Drawings, as originally filed, with Application for Patent Serial No: **2,270,600**, on May 3, 1999, by **INFECTIO RECHERCHE INC.**, assignee of Michel Bergeron, André Désormeaux and Michel J. Tremblay, for "Method and Formulations for the Treatment of Diseases, Particularly Those Caused by Human Immunodeficiency Virus and Leishmania".

PRIORITY DOCUMENT
SUBMITTED OR TRANSMITTED IN COMPLIANCE WITH RULE 17.1(a) OR (b)

Agent certificateur/Certifying Officer

May 23, 2000
Date

Canada

(CIPO 68)

OPIC CIPO

ABSTRACT OF THE DISCLOSURE

The present invention relates to formulations of liposomes and immunoliposomes and method for use in the treatment of diseases, particularly for the treatment of infections caused by viruses such as human immunodeficiency virus and parasites such as leishmania.

TITLE OF THE INVENTION

METHOD AND FORMULATIONS FOR THE TREATMENT OF DISEASES, PARTICULARLY THOSE CAUSED BY HUMAN IMMUNODEFICIENCY VIRUS AND LEISHMANIA

FIELD OF THE INVENTION

This invention relates to formulations of liposomes and immunoliposomes and method for use in the treatment of diseases, particularly for the treatment of infections caused by viruses such as human immunodeficiency virus and parasites such as leishmania.

BACKGROUND OF THE INVENTION

It is now well-established that in the early-stage of human immunodeficiency virus (HIV) infection and throughout the clinical latent stage, HIV accumulates and replicates actively in lymphoid organs despite of a low viral load in peripheral blood. The high viral load observed in the lymphoid tissues was reported to be partly associated with trapped HIV particles on the follicular dendritic cells (FDC) located in the germinal centers. In addition to the extracellular localization of HIV in interdendritic spaces of germimal centers, viral particles are also found within the endosomal and cytoplasm compartments of FDC. Moreover, viral particles bound to the FDC remained highly infectious to CD4+ T-cells despite the presence of neutralizing antibodies on their surface. Over the course of HIV infection, the FDC network was shown to be gradually disrupted and ultimately destroyed. The incapacity of FDC to retain HIV particles in advanced stages of the disease has been postulated to contribute to the increased viral burden in the periphery. As the microenvironment of lymphoid tissues is crucial for effective immune responses, it is important to decrease viral burden and inhibit virus replication at the earliest possible time after infection.

Highly active antiretroviral therapy (HAART), usually consisting of a combination of two nucleoside analogues and one protease inhibitor, has been shown to reduce the plasma viral load in HIV-infected individuals. However, these anti-HIV agents have no effect on free viral particles and they do not fully eliminate viral replication in secondary lymphoid tissues. Studies have established that replicative-competent HIV-1 is routinely isolated from resting CD4+ T-cells from patients receiving HAART even after 30 months of therapy (Chun et al., 1997, Proc. Natl. Acad. Sci. USA 94:13193-13197; Wong et al., 1997, Science 278:1291-1295; Finzi et al., 1997, Science 278:1295-1300). In addition, it was recently shown that initiation of HAART in infected individuals, as early as 10 days after the onset of symptoms of primary

HIV-1 infection, did not prevent generation of latently infected resting CD4+ T-cells carrying integrated HIV-1 DNA despite the successful control of plasma viremia (Chun et al., 1998; Proc. Natl. Acad. Sci. USA 95:8869-8873). On the other hand, increasing numbers of treatment failures resulting from toxicity, drug-resistant mutants and/or poor compliance of patients to drug regimen are emerging with long-term therapy. These is thus a need to develop new strategies to increase the concentration of drugs into lymphoid organs in order to improve the efficacy and safety of antiretroviral agents.

One common feature of retroviruses, as well as of many other enveloped viruses, is the acquisition of host cell surface molecules during the budding process. For example, HIV-1 and HIV-2 have been shown to incorporate a vast array of cell membrane derived structures while budding out of the infected cell. CD4+ T lymphocytes represent the major cellular reservoir for HIV-1 in the peripheral blood and their activation result in upregulation of viral replication. FDC, B lymphocytes, antigen presenting cells like macrophages and activated CD4+ T-cells are abundant in lymphoid tissues and all express substantial levels of the HLA-DR determinant of the major histocompatibility complex class II (MHC-II). Monocyte-derived macrophages, which are also CD4+ and express HLA-DR, are considered to be the most frequently identified hosts of HIV-1 in tissues of infected individuals. Consequently, the probability that newly formed virions will bear cellular HLA-DR is high. More importantly, it has been demonstrated that plasma HIV-1 isolates from virally-infected individuals do carry on their surface host-encoded HLA-DR (Saarloos et al., 1997, J. Virol. 71:1640-1643). The physiological relevance of cellular HLA-DR bound to HIV-1 is further provided by previous studies from our laboratory indicating that HLA-DR is one of the most abundant host-derived molecules carried by HIV-1 (Tremblay et al., 1998, Immunol. Today 19:346-351).

Considering that HIV accumulates and replicates actively within lymphoid tissues, any strategy that will decrease viral stores in these tissues might be beneficial to the infected host. As liposomes are naturally taken up by cells of the mononuclear phagocytic system (MPS), liposome-based therapy represents a convenient approach to improve the delivery of anti-HIV agents within lymphoid tissues. As host-derived HLA-DR proteins are abundantly expressed on antigen presenting cells such as monocyte/macrophages and FDC, liposomes bearing surface-attached anti-HLA-DR antibodies (immunoliposomes) and containing anti-HIV agents constitute a convenient approach to target even more specifically HIV reservoirs. Furthermore, as host-encoded HLA-DR determinant is also present on the virion's surface, incorporation of

neutralizing agents, such as amphotericin B, in anti-HLA-DR immunoliposomes represents an attractive strategy to destroy both free viruses and virally-infected cells.

In addition to treatment of viral diseases, liposome technology can be used for the treatment of other diseases including parasitic diseases. Leishmaniasis refers to diseases caused by the protozoa *Leishmania* spp. Leishmania live in macrophages as intracellular amastigotes in humans and other mammalian hosts, and as extracellular prosmatigotes in the gut of their invertebrate sandfly vectors. Leishmanial infections take three main clinical forms: visceral, cutaneous and mucosal. The high prevalence of leishmaniasis and the emergence of resistance to conventional drugs demonstrate the urgent need to develop new efficient drugs. Camptothecin is a topoisomerase I inhibitor which interferes with the replication of this parasite *in vitro*. However, camptothecin is highly cytotoxic and is rapidly transformed *in vivo* to its carboxylate form that is inactive. Since liposomes are naturally taken up by spleen and liver, which are the major infected organs in visceral leishmaniasis, their use should concentrate drugs into the parasitized host cells. Furthermore, camptothecin incorporated into liposomes should protect its active lactone ring against biological environment.

Our international publication (US patent 5,773,027) discloses the use of antiviral agents encapsulated into liposomes for the treatment of viral diseases. However, this publication does not specifically teach that drugs can be incorporated within liposomes bearing surface-attached anti-HLA-DR antibodies to inhibit replication or destroy both cell-free HIV virions and virus-infected cells. Such anti-HLA-DR immunoliposomes could represent a novel therapeutic strategy to treat more efficiently this debilitating retroviral disease. Furthermore, this publication does not specifically teach the use of camptothecin as a new potential drug for the treatment of leishmaniasis.

SUMMARY OF THE INVENTION

This invention relates to a method for the treatment of diseases comprising the administration of drugs encapsulated into liposomes bearing surface-attached antibodies. This invention also relates to formulations of liposomes bearing surface-attached antibodies for the treatment of viral diseases and more particularly for the treatment of infections caused by HIV. This invention also relates to a method for the treatment of parasitic diseases comprising the administration of drugs encapsulated into liposomes. This invention also relates to formulations of liposomes for the treatment of parasitic diseases and more particularly for the treatment of infections caused by Leishmania.

In a preferred embodiment, formulations of liposomes are composed of dipalmitoylphosphatidylcholine (DPPC):dipalmitpoylphosphatidylglycerol (DPPG) in a molar ratio of 10:3 (thereafter called conventional liposomes). In another preferred embodiment, formulations of liposomes are composed of DPPC:DPPG:distearoylphosphatidylethanolamine-polyetheneglycol (DSPE-PEG) in a molar ratio of 10:3:0.83 (thereafter called stealth liposomes). In still another preferred embodiment, formulations of liposomes are composed of DPPC:DPPG:dipalmitoylphosphatidylethanolamine-N-(4-(p-maleimidophenyl)butyryl) (DPPE-MPB) in a molar ratio of 10:3:0.33 bearing anti-HLA-DR Fab' fragments (thereafter called anti-HLA-DR immunoliposomes or immunoliposomes). In another preferred embodiment, formulations of liposomes are composed of DPPC:DPPG:distearoylphosphatidylethanolamine:N-(4-(p-maleimidophenyl)butyryl) (DSPE-MPB) in a molar ratio of 10:3:0.83 bearing anti-HLA-DR Fab' fragments (thereafter also called anti-HLA-DR immunoliposomes or immunoliposomes). In still another preferred embodiment, formulations of liposomes are composed of DPPC:DPPG:DSPE-polyethyleneglycol-MPB (DSPE-PEG-MPB) in a molar ratio of 10:3:0.83 bearing anti-HLA-DR Fab' fragments (thereafter called stealth anti-HLA-DR immunoliposomes or stealth immunoliposomes). In still another preferred embodiment, formulations of liposomes are composed of DPPC:DPPG:DSPE-PEG-MPB in a molar ratio of 10:3:0.83 bearing anti-HLA-DR Fab' fragments and contains indinavir as an antiviral drug. In another preferred embodiment, formulations of liposomes are composed of DPPC:DPPG in a molar ratio of 10:3 and contains amphotericin B as a drug. In still another preferred embodiment, formulations of liposomes are composed of DPPC:DPPG:DSPE-MPB in a molar ratio of 10:3:0.33 bearing anti-HLA-DR Fab' fragments and contains amphotericin B as a drug. In another preferred embodiment, formulations of liposomes are composed of DPPC:DPPG in a molar ratio of 10:3 and contains campthotecin as a drug.

The above formulations could further comprise a drug which is effective to treat any disease. Liposomes could contain any drug which is effective against the said disease. For the purpose of the invention, the term "drug" is intended to cover any antimicrobial, bactericidal, virucidal, chemotherapeutic, antiinflammatory, antineoplastic, immunomodulator or any other agent or combination of them which is effective for the treatment of the disease. The term "drug" also refers to cytokines or antigens that could stimulate an immune response that would lead to an improved treatment against the said disease.

BRIEF DESCRIPTION OF THE FIGURES

Figure 1 shows flow cytometry scans of A) SUP-T1, B) HUT-78 and C) RAJI cells incubated with conventional liposomes (solid lines) and liposomes bearing anti-HLA-DR (IgG_1, clone 2.06) Fab' fragments (dotted lines) for 30 min at 37°C and revealed with a goat-anti-mouse-FITC-IgG.

Figure 2 shows the effect of liposomal concentration on the binding level of human anti-HLA-DR immunoliposomes with B lymphocytes as revealed by FITC conjugated goat anti-mouse IgG which binds to Fab' fragments (O) and by a fluorescent lipophilic DiI marker incorporated within the lipid membrane of immunoliposomes (●).

Figure 3 shows the tissue distribution of conventional liposomes (dotted bar) and anti-HLA-DR (IgG_{2b}, clone Y-17) immunoliposomes (solid bar) in A) brachial lymph nodes, B) cervical lymph nodes, C) liver and D) spleen following a single subcutaneous injection to mice. Values represent the mean (±SEM) obtained for six animals per group per time point. *Significantly different ($p<0.01$) when compared to conventional liposomes.

Figure 4 shows the tissue distribution of conventional immunoliposomes (dotted bar) and stealth immunoliposomes (solid bar) in brachial, cervical, mesenteric, inguinal and popliteal lymph nodes, and spleen following a single subcutaneous injection to mice. Values represent mean (±SEM) obtained for six animals per group per time point. *, **Significantly different ($p<0.05$) and ($p<0.01$), respectively when compared to conventional immunoliposomes.

Figure 5 shows the tissue distribution of conventional liposomes (empty bar), stealth liposomes (lined bar), conventional immunoliposomes (dotted bar) and stealth immunoliposomes (solid bar) in brachial, cervical, mesenteric, inguinal and popliteal lymph nodes, and spleen following a single subcutaneous injection to mice. Values represent the mean (±SEM) obtained for six animals per group per time point. *Significantly different ($p<0.05$) when compared to conventional liposomes and **significantly different ($p<0.05$) when compared to conventional immunoliposomes.

Figure 6 shows fluorescent micrographs of brachial lymph nodes of C3H mouse at 120 h after the administration of a single subcutaneous dose of Di-I stealth liposomes (Panel A) and stealth immunoliposomes (Panel C) to mice. Panels B and D represent the corresponding

hematoxylin eosin coloration of tissues. Figure shows the cortex area (C), the parafollicular area (PF), the medulla (M) and the lymphoïd follicules (LF). Magnification: 250X.

Figure 7 shows fluorescent micrographs of spleen of C3H mouse at 48 h after the administration of a single subcutaneous dose of Di-I stealth liposomes (Panel A) and stealth immunoliposomes (Panel C) to mice. Panels B and D represent the corresponding hematoxylin eosin coloration of tissues. Figure shows the red pulp (RP) and the marginal zone (M) surrounding lymphoïd follicule of the white pulp (WP). Magnification: 250X.

Figure 8 shows the tissue distribution of free indinavir and anti-HLA-DR immunoliposomes-encapsulated indinavir at different time intervals after a single subcutaneous administration to mice. Panels A, C, E correspond to the concentration of free indinavir (dotted bar) and of indinavir encapsulated in anti-HLA-DR immunoliposomes (solid bar) in cervical, brachial and mesenteric lymph nodes, respectively. Panels B, D, F correspond to the concentration of liposomal lipids in cervical, brachial and mesenteric lymph nodes, respectively. Values represent the mean (±SD) obtained for six animals per group per time point. *, **Significantly different ($p<0.05$) and ($p<0.01$), respectively when compared to free indinavir.

Figure 9 shows the tissue distribution of free indinavir and anti-HLA-DR immunoliposomes-encapsulated indinavir at different time intervals after a single subcutaneous administration to mice. Panels A, C, E correspond to the concentration of free indinavir (dotted bar) and of indinavir encapsulated in anti-HLA-DR immunoliposomes (solid bar) in inguinal lymph nodes, popliteal lymph nodes, and spleen, respectively. Panels B, D, F correspond to the concentration of liposomal lipids in inguinal lymph nodes, popliteal lymph nodes, and spleen, respectively. Values represent the mean (±SD) obtained for six animals per group per time point. *, **Significantly different ($p<0.05$) and ($p<0.01$), respectively when compared to free indinavir.

Figure 10 shows the plasma concentration of free indinavir and anti-HLA-DR immunoliposomes-encapsulated indinavir at different time intervals after a single subcutaneous administration to mice. Panel A corresponds to the plasma concentration of free indinavir (dotted bar) and of indinavir encapsulated in anti-HLA-DR immunoliposomes (solid bar). Panel B corresponds to the plasma concentration of liposomal lipids. Values represent the

mean (±SD) obtained for six animals per group per time point. **Significantly different ($p<0.01$) when compared to free indinavir.

Figure 11 shows the anti-HIV efficacy of different concentrations of free indinavir (dotted bar) and anti-HLA-DR immunoliposomes-encapsulated indinavir (solid bar) in 1G5 cells. Uninfected cells and infected untreated cells were used as control.

Figure 12 shows the effect of free AmB, empty conventional liposomes, liposome-encapsulated AmB, empty immunoliposomes and anti-HLA-DR immunoliposome-encapsulated AmB with respect to infection with HLA-DR-positive HIV-1 particles (strain NL4-3) in the presence of 5 µg AmB/ml (final concentration).

Figure 13 shows the effect of different concentrations of free AmB (empty square) and anti-HLA-DR immunoliposome-encapsulated AmB (solid square) on HIV-1 NL4-3 HLA-DR-positive (Panel A) and NL4-3 HLA-DR-negative (Panel B) replication.

Figure 14 shows the effect of free AmB and anti-HLA-DR immunoliposome-encapsulated AmB on HIV-1 ADA-M HLA-DR-negative replication. (concentration = 5 µg AmB/ml).

Figure 15 shows the uptake of free camptothecin (O) and liposomal camptothecin (●) by B10R macrophages as a function of time. Values represent the mean (±SEM) of three determinations. Results are expressed as µmoles of camptothecin/µg of protein.

Figure 16 shows the number of *Leishmania donovani* units in liver of Balb/C mice infected intravenously with *Leishmania donovani* and treated with intraperitoneal administration of free or liposomal camptothecin (2.5 mg camptothecin/kg). Treatments were given three times a week for two weeks and were initiated either one day (Panel A) or 7 days (Panel B) post-infection. Values represent the mean (±SEM) obtained for six animals per group per time point.

DETAILED DESCRIPTION OF THE INVENTION

The present invention is described herein below by way of specific examples and appended figures, whose purpose is to illustrate the invention rather than to limit its scope.

Drugs

Any antimicrobial, bactericidal, virucidal, chemotherapeutic, antiinflammatory, antineoplastic, immunomodulator or any other agent or combination of them which is effective to treat infection and/or disease is under the scope of this invention. The term "drug" also refers to cytokines or antigens that could stimulate an immune response that would lead to an improved treatment against the said infection and/or disease.

Liposomes

The present invention include liposomes composed of any vesicle-forming lipids. For the purpose of this invention, the term "vesicle-forming lipids" is intented to cover any amphipathic lipid having hydrophobic and polar head group moieties which can form bilayer vesicles in aqueous solutions or can be incorporated into lipid bilayers. Included in this class are phospholipids such as phosphatidylcholine (PC), phosphatidylglycerol (PG), phosphatidylethanolamine (PE), phosphatidylserine (PS), phosphatidylinositol (PI), phosphatidic acid (PA) and sphingomyelin (SM) where the two hydrocarbon chains are typically beteween about 14-22 carbon atoms in length and have varying degrees of unsaturation. Also included in this class are glycolipids, such as cerebrosides and gangliosides. Also included in this class are cholesterol and related sterols. Also included in this class are amphipathic lipids having a derivatized hydrophilic biocompatible polymer such as polyethyleneglycol. The liposomes of the present invention also include immunoliposomes, defined herein as, liposomes which are modified by the coupling of antibody molecules which enhance the targeting of specific cells. The liposomes of the present invention also include pH-sensitive liposomes, heat-sensitive liposomes, target-sensitive liposomes and any other type of liposomes that could be used for this purpose. This invention also covers any combination of liposomes and/or drugs.

The preparation of liposomes in the present invention can be carried out by a variety of techniques such as those described in the literature. Formulations of liposomes of the present invention include those having a mean particle diameter of any size prepared with any drug/lipid molar ratio. Incorporation of drugs into liposomes can be achieved by one or more methods of active and/or passive loading such as those described in the literature. Details for the preparation of liposomes are provided in the following examples.

Examples involving our liposomal formulations for treatment of infection

The following examples are intended to demonstrate the preparation of liposomal formulations that could be efficient to treat infection caused by any pathogen and/or any disease, but are in no way intended to limit the scope thereof.

Preparation of anti-HLA-DR immunoliposomes

Hybridomas producing monoclonal antibodies directed against human (clone 2.06, IgG_1) and murine (clone Y-17, IgG_{2b}) HLA-DR were obtained from the American Type Culture Collection (Rockville, MD). Antibodies were isolated from ascites fluids of BALB/c mice and purified using a protein-G affinity column. Antibodies were sterilized on 0.22 µm low binding protein filters and stored at -20°C in phosphate buffered saline (PBS, pH 7.4). Purity of antibodies was assessed by sodium dodecyl sulfate polyacrylamide gel electrophoresis (SDS-PAGE) under non-reducing conditions.

$F(ab')_2$ fragments of antibody 2.06 were produced using an Immunopure IgG_1 Fab' and $F(ab')_2$ preparation kit (Pierce, Rockford, IL). In brief, the 2.06 antibody was concentrated with a Centricon-100 (Amicon, Beverly, MA), resuspended in 0.5 ml of PBS and added to 0.5 ml of Immunopure IgG_1 mild elution buffer containing 1 mM cysteine. The solution was then incubated with an immobilized ficin column for 40 h at 37°C. The solution was then eluted with 4 ml of Immunopure binding buffer and fragments were separated on an Immunopure protein A column. The column retained Fc fragments and undigested IgG_1 whereas $F(ab')_2$ fragments were collected. Fractions containing $F(ab')_2$ were determined from absorbance readings at 280 nm and pooled together. The $F(ab')_2$ fragments (110 kD) were then concentrated using Centricon-50 and resupended in phosphate-EDTA buffer (100 mM sodium phosphate and 5 mM EDTA, pH 6.0). $F(ab')_2$ fragments of antibody Y-17 were produced following incubation of the antibody with lysyl endopeptidase (in 50 mM Tris-HCl, pH 8.5) in an enzyme/substrate molar ratio of 1:50 for 3 h at 37°C. Lysyl endopeptidase cleaved IgG_{2b} at Lys 228E/Cys 229 without perturbing disulfide bridges. The digestion products contained undigested IgG, $F(ab')_2$ and Fc fragments. The enzyme was removed by gel chromatography on a Sephadex G-25M column and fragments were fractionnated with a protein A affinity chromatography column and resupended in phosphate-EDTA.

$F(ab')_2$ fragments were incubated with of 2-mercaptoethylamine-HCl (MEA, final concentration of 0.05 M) for 90 min at 37°C under nitrogen atmosphere. MEA cleaved the disulfide bridges between the heavy chains but preserved the disulfide linkages between the

heavy and light chains. The solution was eluted on a Sephadex G-25M column pre-equilibrated with acetate-EDTA buffer (100 mM anhydrous sodium acetate, 88 mM sodium chloride and 1 mM EDTA, pH 6.5) and Fab' fragments were collected. Fractions containing Fab' were determined using a BCA protein assay reagent kit (Pierce, Rockford, IL) and pooled together. Fab' fragments (55 kD) were concentrated using Centricon-10, resuspended in acetate-EDTA buffer (pH 6.5) and kept under nitrogen atmosphere at 4°C until coupling to liposomes. The purity of Fab' fragments was assessed by SDS-PAGE and their antigenic specificity was verified by flow cytometry using appropriate cells.

Liposomes composed of DPPC/DPPG/DPPE-MPB, DPPC/DPPG/DSPE-MPB and DPPC/DPPG/DSPE-PEG-MPB were prepared according to the method of thin lipid film hydration. In brief, the lipid mixture was dissolved in chloroform in a round-bottomed flask and the organic solvent was evaporated to form a thin lipid film. In some experiments, [^{3}H]-cholesterylhexadecylether was added as a radioactive tracer. The lipid film was then hydrated with an acetate-EDTA buffer (pH 6.5). Multilamellar vesicles (MLVs) were sequentially extruded through polycarbonate membranes of defined pore sizes (Nuclepore, Cambridge, MA) using a stainless steel extrusion device (Lipex Biomembranes, Vancouver, BC). The final concentration of liposomes was determined using an enzymatic colorimetric method.

Freshly prepared liposomes were incubated with freshly prepared Fab' fragments overnight at 4°C under continuous agitation and under nitrogen atmosphere. Liposomes-bearing surface attached antibodies (immunoliposomes) were separated from unconjugated Fab' fragments by ultracentrifugation (100 000 x g, twice for 45 min at 4°C) and immunoliposomes were resuspended in PBS (pH 7.4). The total amount of Fab' conjugated to liposomes was evaluated with the Coomassie protein assay reagent (Pierce, Rockford, IL).

Even though the following examples describe specific liposomal formulations, it is deemed that a family of liposomal formulations can be easily derived therefrom, without affecting the valuable properties thereof. Formulations of liposomes of the present invention include those having a mean particle diameter of any size. The formulations of liposomes of the present invention also include those prepared with any drug/lipid molar ratio. The following examples are intended to demonstrate specific liposomal formulations of drugs which could be very efficient for the treatment of infections caused by HIV and Leishmania, but are in no way intended to limit the scope thereof.

***In vitro* binding and specificity of immunoliposomes**

The binding and specificity of conventional liposomes and anti-HLA-DR immunoliposomes were evaluated in RAJI, HUT-78 and SUP-T1 cells by flow cytometry assay. In brief, cells were maintained in complete culture medium of RPMI 1640 supplemented with 10% fetal bovine serum, 2 mM glutamine, 100 U/ml penicillin G and 100 µg/ml streptomycin at 37°C under a 5% CO_2 atmosphere. Cells (5 x 10^5 cells/ml) suspended in PBS were incubated with 1.5 µmol of conventional liposomes or immunoliposomes for 30 min on ice or at 37°C and washed three times with PBS. DiI-labelled (immuno)liposomes were incubated with PBS whereas DiI-free (immuno)liposomes were stained with FITC conjugated goat anti-mouse IgG at a dilution of 1:50. Samples were washed with PBS and resuspended in 1% paraformaldehyde. The specificity of liposomes for the cells was determined by flow cytometry from the fluorescence associated to DiI (fluorochrome incorporated into the lipid membrane) and to FITC (fluorochrome associated to Fab' fragments). The effect of liposomal concentration on the binding level of immunoliposomes to RAJI cells has also been evaluated according to the protocol described above.

Figure 1 shows the levels of binding of conventional liposomes and human anti-HLA-DR (IgG_1, clone 2.06) immunoliposomes to three human lymphoma cell lines expressing different surface levels of the human HLA-DR determinant of MHC-II revealed by flow cytometry. As expected, anti-HLA-DR immunoliposomes did not bind to SUP-T1 cells that does not express HLA-DR on their surface (Panel A). In contrast, a very strong binding was observed following incubation of liposomes bearing anti-HLA-DR with both the HUT-78 and RAJI cells (Panels B and C) which bear important levels of human HLA-DR on their surface. These results clearly showed that liposomes bearing human anti-HLA-DR Fab' fragments were very specific to cells expressing HLA-DR determinant of MHC-II. The specificity of murine anti-HLA-DR immunoliposomes for I-E antigens present on mouse spleen cells has also been confirmed using a similar technical approach (data not shown).

The effect of liposomal concentration on the levels of binding of human anti-HLA-DR immunoliposomes on B lymphocytes has also been investigated using two different fluorescent markers: i) a goat anti-mouse IgG (FITC) which binds to Fab' fragments and ii) a fluorescent lipophilic DiI marker incorporated within the lipid membrane of immunoliposomes. Results showed that the binding level of immunoliposomes with B cells, when incubated at 37°C, was rapidly saturated when using FITC conjugated goat anti-mouse IgG as a marker whereas it increased linearly over the lipid concentration range when considering the fluorescence signal

associated to DiI (figure 2). The saturation effect observed in the binding level of immunoliposomes using FITC as a marker is attributed to the fact that a constant concentration of FITC-IgG was used for all liposomal concentrations used. In contrast, as DiI is located in the lipid bilayer of immunoliposomes, the fluorescence intensity level was proportional to the lipid concentration used. Similar results were also obtained for the *in vitro* binding experiments performed at 4°C (data not shown). Data were presented only for incubation of cells with immunoliposomes at 37°C as they are representative of *in vivo* conditions.

Tissue distribution studies

The accumulation of conventional and murine anti-HLA-DR immunoliposomes within lymphoïd and non-lymphoïd tissues has been investigated in mice. In brief, a single bolus injection of conventional liposomes, stealth liposomes, conventional immunoliposomes or stealth immunoliposomes containing a small amount of radioactive lipid was administered subcutaneously in the upper back below the neck of female C3H mice (18-20 g; Charles River Breeding Laboratories, St-Constant, QC). At specific time, animals were sacrificed and blood was collected and separated by centrifugation (6000 x g for 10 min at 4°C). At the same time, selected tissues were collected, washed in PBS and weighed. Tissues and plasma were then treated with tissue solubilizer and decoloured in H_2O_2. Lipid levels in all samples were monitored by counting radioactivity. Six animals were used for each time point.

Figure 3 shows the tissue distribution of conventional liposomes and anti-HLA-DR immunoliposomes in cervical lymph nodes, brachial lymph nodes, liver and spleen at different time intervals post-injection. Liposomes bearing murine anti-HLA-DR Fab' fragments targeted more efficiently the cervical lymph nodes when compared to that of conventional liposomes with a peak accumulation at 24 h post-injection. The accumulation of anti-HLA-DR immunoliposomes within brachial lymph nodes was very similar to that of conventional liposomes in the first 12 h post injection but was significantly higher at 24 and 48 h post-injection. The concentration of anti-HLA-DR immunoliposomes within the liver was significantly lower than that of conventional liposomes for the first 12 h post-injection but reached similar values at 24 and 48 h post-administration whereas a lower accumulation of immunoliposomes was observed in the spleen for all time points studied.

Table 1 shows the area under the curve of anti-HLA-DR immunoliposomes and conventional liposomes in these different tissues. When compared to conventional liposomes, the subcutaneous administration of anti-HLA-DR immunoliposomes resulted in a 2.9 and 1.6

times greater accumulation in the cervical and brachial lymph nodes, respectively. On the other hand, the liposomal accumulation in the liver was similar for both liposomal preparations, whereas an approximately two-fold decreased accumulation was observed for immunoliposomes in the spleen. In addition, results clearly showed that the subcutaneous administration route was very efficient for lymph node targeting as evidenced by the much higher accumulation of immunoliposomes in these tissues when compared to that observed in the liver and spleen.

Table 1. Area under the curve of anti-HLA-DR immunoliposomes and conventional liposomes in different tissues following a single subcutaneous administration to C3H mice[a].

Tissues	Immunoliposomes	Conventional liposomes	Ratio immunoliposomes/ conventional liposomes
Cervical lymph nodes	105.04	36.37	2.89
Brachial lymph nodes	61.65	39.20	1.57
Liver	4.03	4.21	0.96
Spleen	3.32	7.65	0.43

[a]Values, expressed in μmoles lipids/g tissue/h, were calculated from the mean values of the tissue distribution profile using the trapezoidal rule.

The coupling of polyethyleneglycol (PEG) on the surface of liposomes (stealth liposomes) is known to increase their ability to move through the lymph after subcutaneous injection and to decrease the rate of uptake into the MPS, increasing their residence time within plasma and/or lymph. Consequently, we have evaluated if attachment of anti-HLA-DR Fab' fragments to the end termini of PEG-coating liposomes (stealth immunoliposomes) could further improve their tissue accumulation compared to stealth liposomes. Results showed that the concentration of both immunoliposomal formulations was higher in brachial and cervical lymph nodes than in other tissues suggesting that subcutaneous administration of liposomes accumulates preferentially in regional lymph nodes (figure 4). In addition, stealth immunoliposomes targeted more efficiently all tissues, with a peak of accumulation at 240 h in brachial, inguinal and popliteal lymph nodes and at 360 h or greater for cervical lymph nodes. Their was no significant differences in the accumulation of stealth and conventional

immunoliposomes at 6 h post-injection in lymph nodes and spleen, except for the popliteal lymph nodes, which are the farther lymph nodes from the injection site. The concentration of stealth immunoliposomes in mesenteric lymph nodes reached a plateau at 24 h post-injection and the tissue distribution profile was similar to that observed in the spleen.

Table 2 shows the area under the curve of conventional and stealth immunoliposomes in different tissues. Results clearly demonstrated that stealth immunoliposomes accumulate much better than conventional immunoliposomes in all tissues indicating that the presence of PEG has an important effect on the uptake of immunoliposomes by the lymphatic system.

Table 2. Area under the curve of stealth immunoliposomes and conventional immunoliposomes in different tissues, following the administration of a single subcutaneous dose to C3H mice.[a]

Tissues	Stealth-immunoliposomes	Conventional immunoliposomes	Ratio conv. immuno/ stealth immuno
Cervical lymph nodes	1514.7	616.1	2.46
Brachial lymph nodes	1693.7	874.7	1.94
Mesenteric lymph nodes	16.0	5.5	2.91
Inguinal lymph nodes	34.8	15.8	2.20
Popliteal lymph nodes	70.8	26.3	2.69
Liver	61.5	25.5	2.41
Spleen	57.4	12.6	4.56

[a]Values, expressed in µmoles lipids/g tissues/h, were calculated from the mean values of the tissue distribution profile using the trapezoidal rule.

In another experiment, the concentration of the four types of liposomes (conventional liposomes, stealth liposomes, conventional immunoliposomes and stealth immunoliposomes) was determined at 48 and 120 h after their subcutaneous administration to C3H mice. Results showed that the presence of PEG on the surface of liposomes or immunoliposomes had no effect on their lymphatic uptake in regional lymph nodes (brachial and cervical), but significantly increased their accumulation in other lymph nodes compared to conventional

liposomes or immunoliposomes (figure 5). On the other hand, there was no significant difference in the accumulation of stealth liposomes in the spleen when compared to conventional liposomes. In contrast, the concentration of stealth immunoliposomes was much higher in the spleen when compared to conventional immunoliposomes. In addition, results showed that the presence of anti-HLA-DR Fab' fragments on both conventional and stealth liposomes greatly improved their accumulation in regional lymph nodes when compared to non-targeted liposomes.

Since stealth liposomes and stealth immunoliposomes represent the best formulations to target lymphoid tissues, we have next evaluated if the presence of anti-HLA-DR Fab' fragments at the end termini of PEG chains affect the tissue localization of liposomes. In this set of experiments, liposomal lipids (2.5 mg/ml) were first incubated with 10 μg/ml of 1,1'-dioctadecyl-3,3,3'3'-tetramethylindocarbocyanine perchlorate (DiI) under darkness for 1 h at 60°C with agitation. Unbound DiI was removed by centrifugation (300 x g for 15 min at 4°C) of the liposomal preparation through a coarse Sephadex G-50 column. A single bolus injection of stealth liposomes and stealth immunoliposomes was administered subcutaneously in the upper back below the neck of female C3H mice. At specific times post-injection (24, 48 and 120 h), animals were sacrificed and tissues (spleen, brachial and cervical lymph nodes) were removed. Tissues were then washed in PBS, embedded in OCT, frozen in liquid nitrogen and stored at -20°C. Tissue sections of 10 μm thickness were cut using a Jung Figocut 2800E from Leica Canada Inc. (St-Laurent, QC) and deposited on slides pre-treated with 2% aminoalkysilane. Coated slides were immediately observed using a Nikon Microflex HFX-DX fluorescence microscope and pictures were taken with a Nikon camera. Di-I fluorescence was observed with a rhodamine optics excitation filter.

Figure 6 compares the localization of fluorescent stealth liposomes and stealth immunoliposomes in brachial lymph nodes at 48 h after their subcutaneous administration in mice. Results showed that the localization of stealth immunoliposomes was very different from that of stealth liposomes in brachial lymph nodes. Stealth liposomes were mainly localized in the subcapsular area, probably in the afferent lymphatic vessel and around the afferent area. In contrast, stealth anti-HLA-DR immunoliposomes mostly accumulated in the cortex in which follicles (B cells and FDCs) are located and in parafollicular areas in which T-cell, interdigitating dendritic cells and other accessory cells are abundant.

Figure 7 compares the localization of stealth liposomes and stealth immunoliposomes in spleen at 120 h after their subcutaneous administration to mice. Once again, results showed that the accumulation of stealth immunoliposomes is better than stealth liposomes in this tissue but their localization was different. Stealth liposomes were localized mostly in the red pulp and the marginal zone of the white pulp whereas stealth immunoliposomes were largely concentrated in the follicle of the white pulp and little in the marginal zone.

The tissue distribution of indinavir, either as free or encapsulated in stealth immunoliposomes, has also been evaluated after a single subcutaneous administration to C3H mice. Figures 8 and 9 show that the incorporation of indinavir in stealth immunoliposomes strongly altered the tissue distribution of the antiviral agent. At first, a much higher accumulation of the anti-HIV agent incorporated in stealth immunoliposomes was observed in all tissues with a peak level at about 24 h post-injection. In addition, significant levels of immunoliposomal indinavir were observed to up to at least 15 days post-administration. Table 3 shows the area under the curve of free and anti-HLA-DR-immunoliposomes-encapsulated indinavir in the different tissues. Results clearly demonstrated that indinavir incorporated in stealth immunoliposomes accumulated much better than the free agent in all tissues. The incorporation of anti-HIV agents within steaalth-immunoliposomes should concentrate drugs within cells susceptible to HIV infection improving therefore the antiviral efficacy of drugs and reducing thereby their systemic toxicity.

Table 3. Area under the curve of free and anti-HLA-DR immunoliposomes-encapsulated indinavir in different tissues after a single subcutaneous administration to C3H mice[a].

Tissues	Immunoliposomal indinavir	Free indinavir	Ratio immunoliposomal/ free indinavir
Cervical lymph nodes	213.1	7.1	30.1
Brachial lymph nodes	239.1	4.6	52.0
Mesenteric lymph nodes	49.9	6.4	7.8
Inguinal lymph nodes	42.0	3.5	11.9
Popliteal lymph nodes	40.9	4.5	9.2
Spleen	211.3	5.3	39.8

[a]Values, expressed in μmoles lipids/g tissues/h, were calculated from the mean values of the tissue distribution profile using the trapezoidal rule.

Figure 10 shows the plasma concentration time curve of free indinavir and anti-HLA-DR immunoliposomes-encapsulated indinavir after a single subcutaneous administration to C3H mice. The encapsulation of indinavir greatly modified its pharmacokinetic profile. A much longer plasma half-life was observed for indinavir entrapped in stealth-immunoliposomes. Indeed, the free agent was completely eliminated from plasma within few hours, whereas significant drug levels were found for up to 10 days post-injection when indinavir was encapsulated in stealth-immunoliposomes. Such improved pharmacokinetics are of prime importance as it should reduce the frequency of administration of the anti-HIV agent and consequently improving the quality of life of patients.

***In vitro* efficacy studies of free, liposomal and immunoliposomal drugs**

The antiviral efficacy of free indinavir and anti-HLA-DR-immunoliposomes-encapsulated indinavir has been evaluated in 1G5 cells, a derivative of Jurkat E6-1 that contains a stably integrated HIV-1-LTR-driven luciferase construct. In brief, cells were infected with NL4-3 HIV-1 strain (10 ng of p24/10^5 cells) in presence of free or liposomal encapsulated indinavir at a concentration ranging from 0 to 200 nM. Afterwards, cells were allowed to grow for 12 days without any additional treatment. Viral replication was measured by luciferase activity. In brief, 100 µl of cell-free supernatant was withdrawn from each well and 25 µl of 5X cell culture lysis buffer (125 mM Tris phosphate (pH 7.8), 10 mM DTT, 5% Triton X-100, 50% glycerol) was added before incubation at room temperature for 30 min. Thereafter, an aliquot of this cell lysate (20 µl) was mixed with 100 µl of luciferase assay buffer (20 mM Tricine, 1.07 mM $(MgCO_3)_4$ $Mg(OH)_2$ $5H_2$), 2.67 mM $MgSO_4$, 0.1 mM EDTA, 270 µM coenzyme A, 470 µM luciferin, 530 µM ATP, 33.3 mM DTT). Emission of light produced by the reaction was measured using liquid scintillation counter. Total photo events over 50 s were measured. Results from this set of experiments showed that immunoliposomal indinavir was as effective as free indinavir to inhibit HIV-1 replication in this lymphocyte cell line (figure 11). Considering that indinavir accumulated much better in lympoid tissues upon encapsulation within immunoliposomes compared to free drug, it is expected that a better antiviral efficacy will be obtained under *in vivo* conditions.

The level of binding of anti-human-HLA-DR (IgG_1, clone 2.06) immunoliposomes and conventional liposomes to RAJI human lymphoma cell line, expressing high levels of HLA-DR on their surface was also evaluated. As expected, incubation of anti-HLA-DR immunoliposomes, containing or not AmB, resulted in a very strong binding on RAJI cells

(data not shown). In contrast, negligible binding was observed when conventional liposomes, containing or not AmB, were incubated with this cell line. These results clearly demonstrate that anti-HLA-DR Fab' fragments coupled on the surface of liposomes keep their specificity to HLA-DR-positive cells. Consequently, our immunoliposomes will most likely specifically target host-derived HLA-DR molecules.

The efficacy of different formulations of AmB to inhibit HIV-1 replication has also been evaluated in 1G5 cells (HLA-DR-negative) and in the monocytic cell line MONO-MAC-1 (HLA-DR-positive) using T- or macrophage-tropic HIV-1 strains that have incorporated or not host-derived HLA-DR proteins. In brief, NL4-3 HLA-DR-positive, NL4-3 HLA-DR-negative or ADA-M viruses (10 ng of p24) were treated with free AmB, AmB incorporated in conventional liposomes or anti-HLA-DR immunoliposomes, empty conventional liposomes or anti-HLA-DR immunoliposomes (concentration of AmB ranging from 0 to 5 µg/ml), or the corresponding amount of liposomes or immunoliposomes, for 60 min at 37°C, in a final volume of 100 µl of complete culture medium. Afterwards, 1G5 cells (10^5 cells) were infected with equal amounts of pretreated NL4-3 HLA-DR-positive or NL4-3 HLA-DR-negative viruses for 2 h at 37°C, in a final volume of 200 µl of complete culture medium. MONO-MAC-1 cells were infected with ADA-M virus according to the same conditions described above. Cells were then washed with PBS, resuspended in 200 µl of complete culture medium, and transferred in a 96-well flat-bottom tissue culture. After an incubation period of 72 h at 37°C under a 5% CO_2 atmosphere in the absence of AmB or liposomes, luciferase activity was monitored.

Figure 12 shows that pretreatment of HIV_{NL4-3}-HLA-DR-positive with 5 µg AmB/ml, dramatically inhibited its infectivity in 1G5 cells. Treatment of HIV-1 particles expressing host-encoded HLA-DR with anti-HLA-DR immunoliposome encapsulated AmB was as efficient as free AmB to inhibit HIV-1 replication at this AmB concentration. On the other hand, liposome-encapsulated AmB did not affect HIV infectivity at this concentration suggesting that inhibition of HIV particles by anti-HLA-DR immunoliposomal AmB is potentially due to specific targeting of HLA-DR host embedded molecules. Interestingly, empty anti-HLA-DR immunoliposomes and empty liposomes had no effect on viral replication at the same lipid concentration than liposomal AmB and immunoliposomal AmB (data not shown). These results demonstrate that inhibition of HIV-1 infectivity by immunoliposomes-encapsulated AmB may be due to the combination of liposomal targeting and specific antiviral effect of AmB. Cell viability experiments showed that AmB, liposomes and immunoliposomes

were not toxic to 1G5 cells at a concentration of 5 µg/ml AmB or at the corresponding amount of empty liposomes and immunoliposomes (data not shown).

To investigate whether anti-HLA-DR immunoliposomes-encapsulated AmB can inhibit specifically the infectivity of HIV-1 particles that have incorporated host-derived HLA-DR proteins, NL4-3 HLA-DR-negative and NL4-3 HLA-DR-positive viruses were incubated with different concentrations of free and immunoliposomal AmB. As expected, immunoliposomal AmB had no effect on HIV-1 NL4-3 HLA-DR-negative replication at concentrations ranging from 0 to 5 µg/ml (figure 13). In contrast, anti-HLA-DR immunoliposomes-encapsulated-AmB inhibited 80% of HIV HLA-DR-positive replication at a concentration as low as 0.5 µg AmB/mL In contrast, free AmB had no significant antiviral activity at this concentration. These results confirmed that immunoliposome-encapsulated AmB specifically targets HIV-1 expressing host-derived HLA-DR proteins and inhibits HIV replication more efficiently than free AmB.

The next step was to determined the effect of anti-HLA-DR immunoliposomes-encapsulated AmB on other HIV-1 strains. For that, inhibition of viral replication of a macrophage tropic strain of HIV-1 such as ADA-M with immunoliposome-encapsulated AmB was monitored in HLA-DR-positive cells. Viral particles devoided of host-encoded HLA-DR proteins were treated with the same amount of AmB, either as free or encapsulated into immunoliposomes, and cells were infected for 72 h. Surprisingly, anti-HLA-DR immunoliposomal AmB was as efficient as free AmB to inhibit ADA-M HLA-DR-negative replication in HLA-DR-positive cells, without significant toxicity of both free or immunoliposome-encapsulated AmB (figure 14). These results suggest that anti-HLA-DR immunoliposomal AmB could have a protective effect against virus infection in HLA-DR-positive cells by drug accumulation after specific targeting of HLA-DR molecules expressed on cells.

Studies involving liposomal camptothecin

The uptake of free and liposomal camptothecin has been evaluated in B10R macrophages. In brief, free or liposomal camptothecin, containing a small amount of radiolabelled drug, was incubated with B10R cells for differents times (0.5, 1, 2 and 4 h) at 37°C. Cells were then washed with PBS and lysed with a detergent. The concentration of incorporated drug within cells was evaluated by measuring radioactivity. The concentration of cellular proteins was evaluated using a BCA protein assay reagent kit. Results showed that

camptothecin incorporated into liposomes accumulated much better than the free agent within this cell line (figure 15).

The efficacy of free and liposomal camptothecin against *Leishmania donovani* has been also evaluated in a murine model of leishmania. In brief, BALB/c mice were infected intravenously with 10^7 of *Leishmania donovani* promastigotes. Mice were then treated with free or liposomal camptothecin (2.5 mg camptothecin/kg) given intraperitoneally three times a week for two weeks and initiated either one day or seven days post-infection. Three days after the last treatment, mice were sacrificed and impression smears of liver were made and examined on microscopic slides. The efficacy of treatment was evaluated by counting parasites using optical microscope. Figure 16 showed that treatment of infected mice with both regimens of either free or liposomal camptothecin gave good efficacy against *Leishmania donovani*. We believe that optimizing the drug concentration and/or treatment regimen should result in a better efficacy of the liposomal camptothecin over the free agent.

CLAIMS:

1. A method for treating a patient comprising an administration of a therapeutically effective dose of a drug encapsulated into liposomes, wherein said liposomes bear surface-attached antibodies.

2. A pharmaceutical composition comprising a drug encapsulated into liposomes, wherein said liposomes bear surface-attached antibodies.

Figure 1

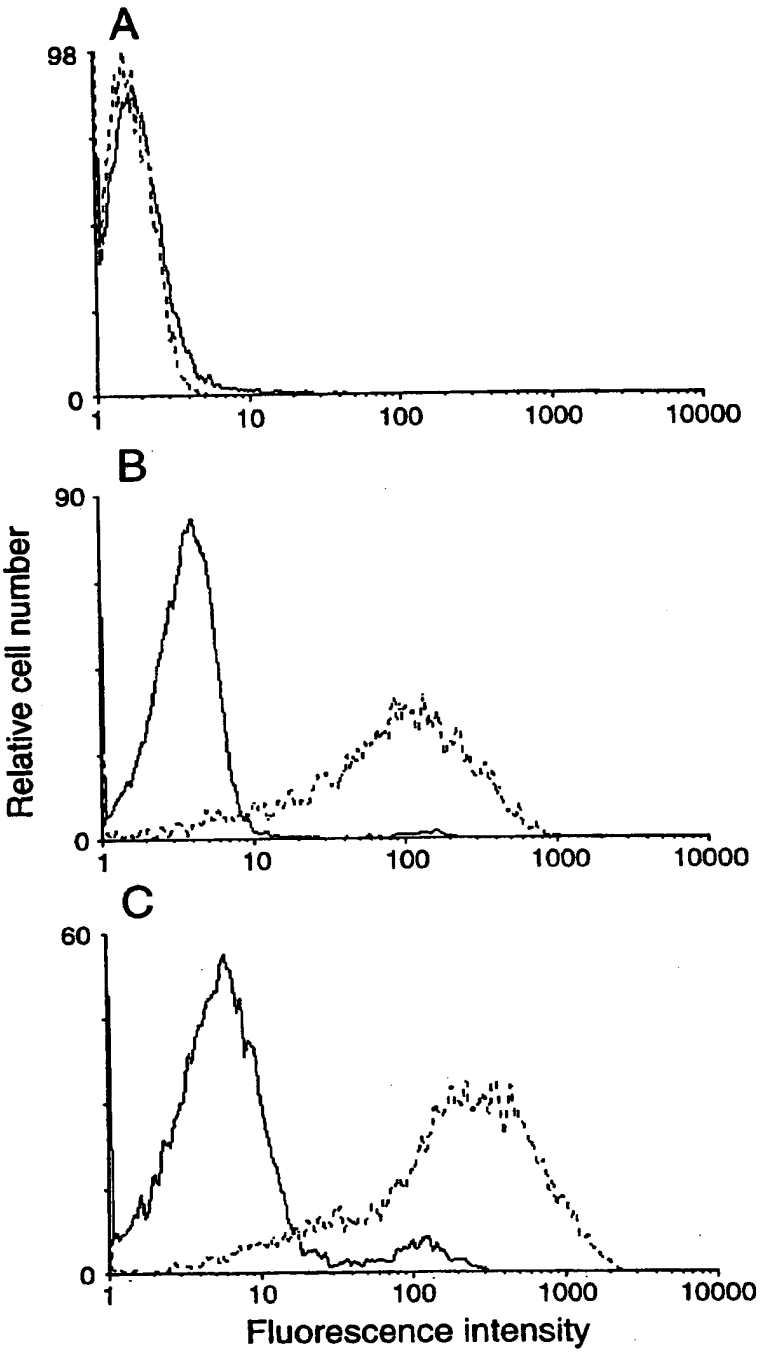
A
98
0
1
10
100
1000
10000
B
90
0
1
10
100
1000
10000
Relative cell number
C
60
0
1
10
100
1000
10000
Fluorescence intensity

Figure 2

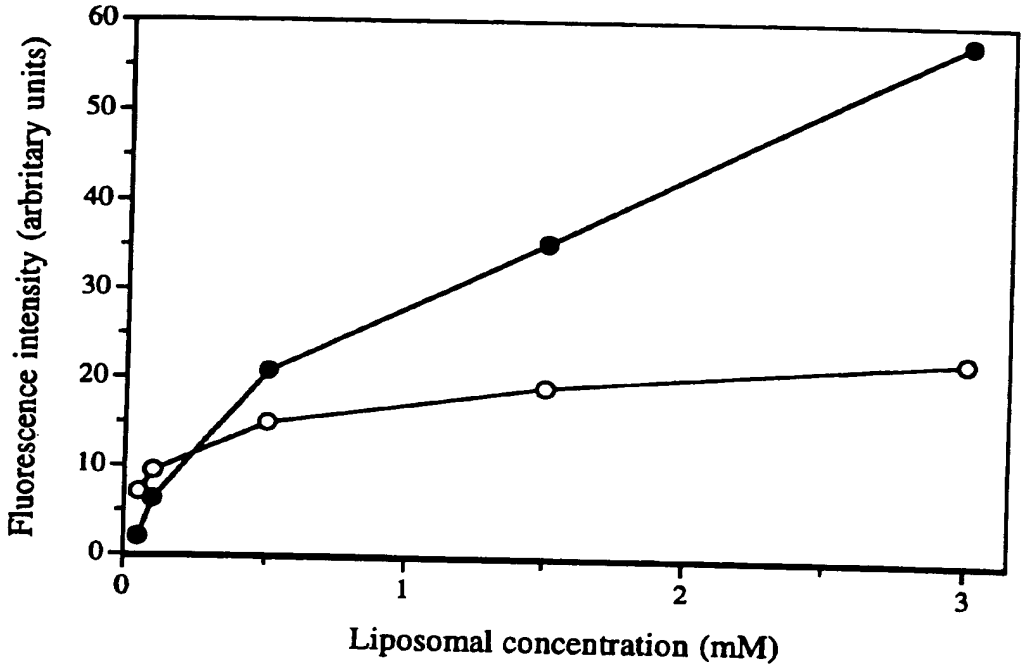
Fluorescence intensity (arbitary units)
60
50
40
30
20
10
0
0
1
2
3
Liposomal concentration (mM)

Figure 3

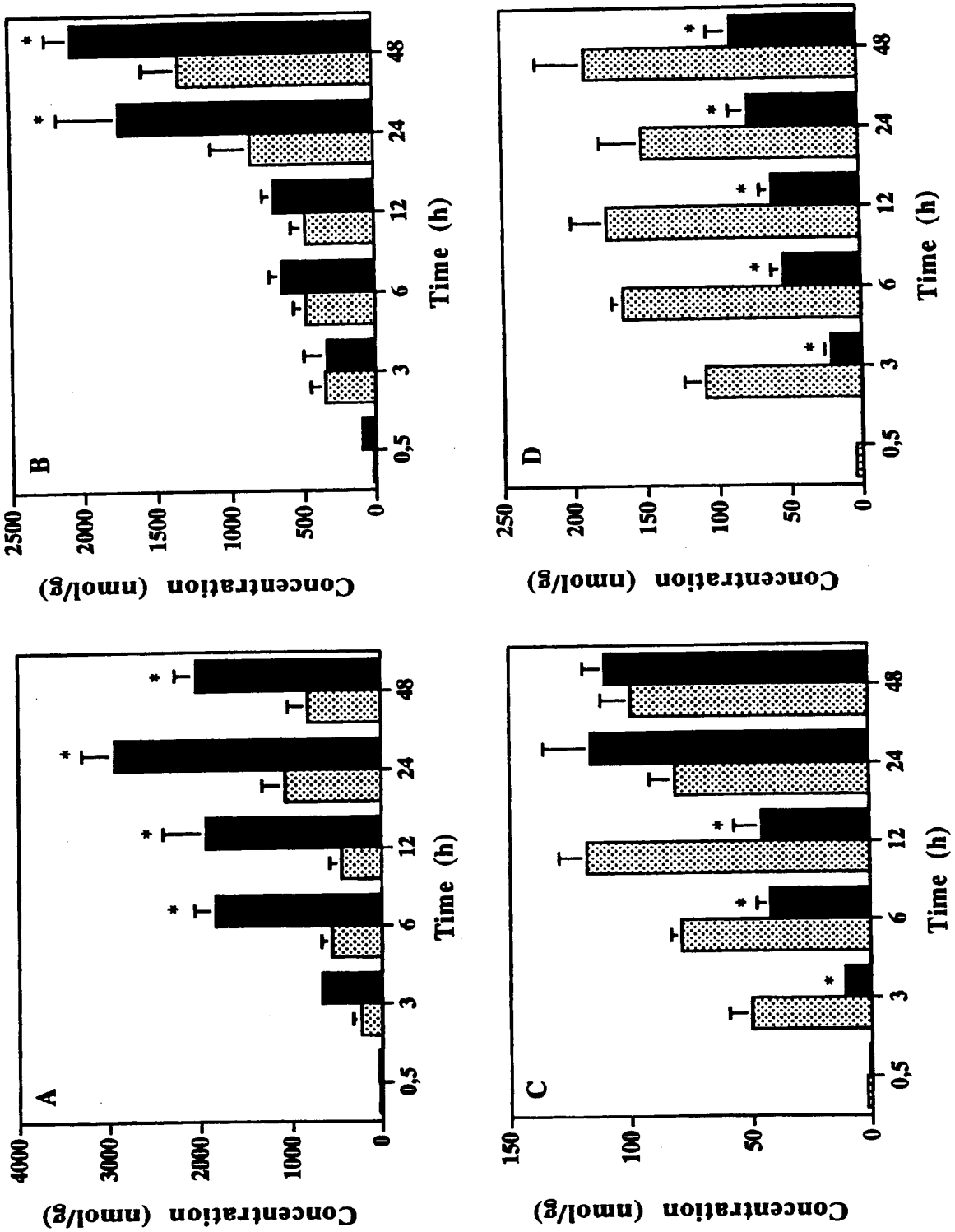
A
B
C
D
Concentration (nmol/g)
Time (h)
0,5
3
6
12
24
48
0
1000
2000
3000
4000
500
1500
2500
50
100
150
200
250
*
T
-

Figure 4

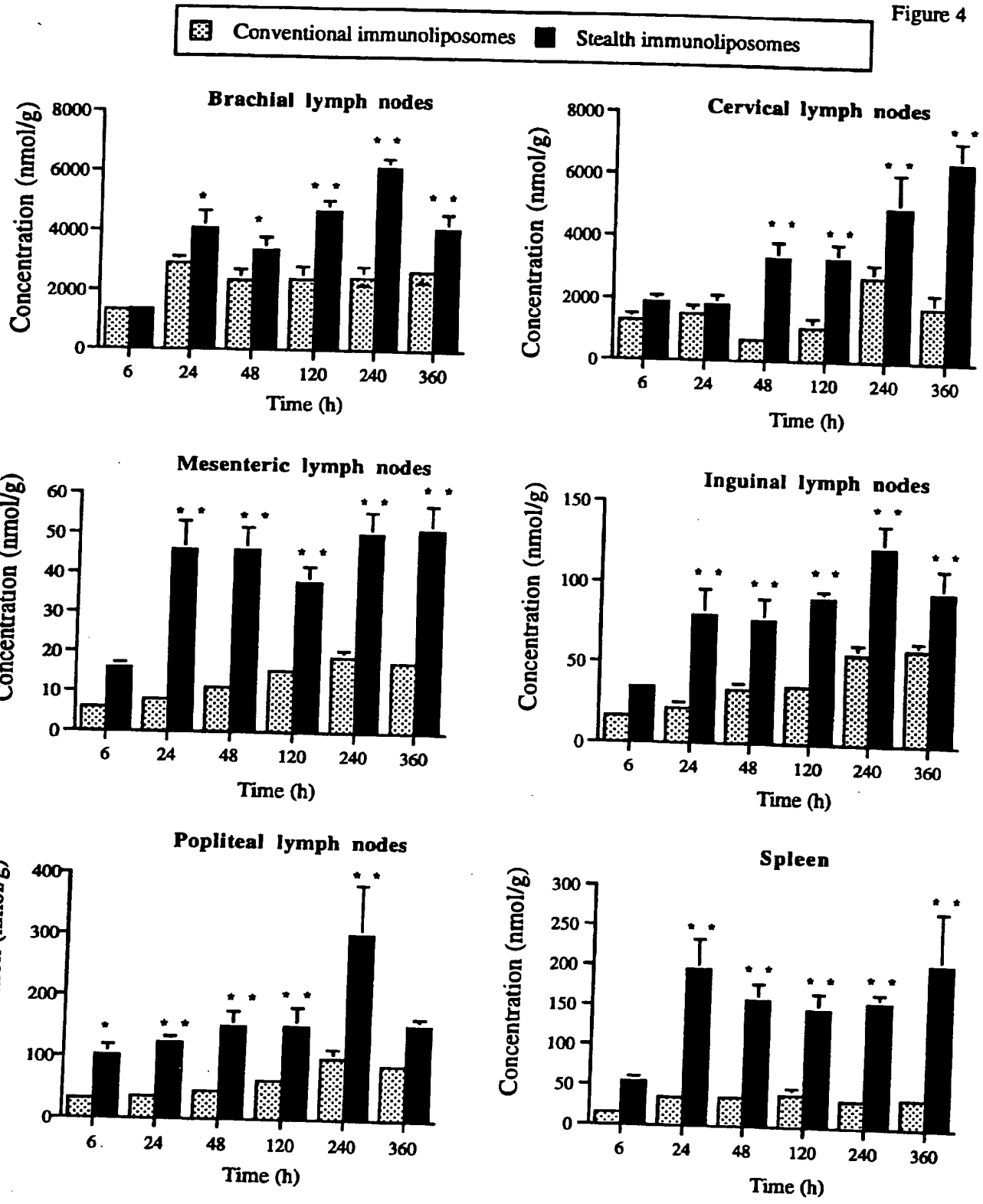
Conventional immunoliposomes
Stealth immunoliposomes
Brachial lymph nodes
Cervical lymph nodes
Mesenteric lymph nodes
Inguinal lymph nodes
Popliteal lymph nodes
Spleen
Concentration (nmol/g)
Time (h)
6
24
48
120
240
360

Figure 5

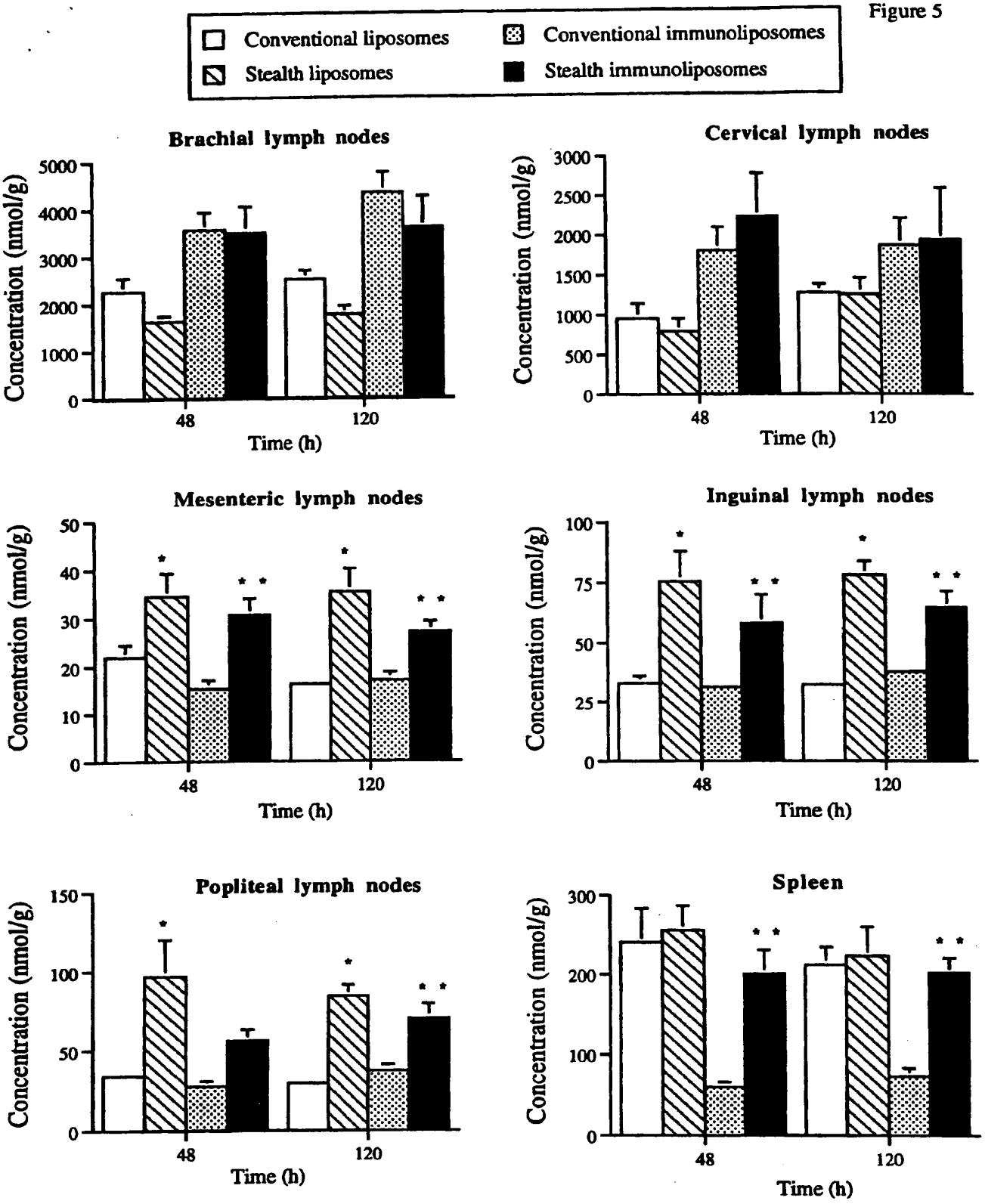
Conventional liposomes
Conventional immunoliposomes
Stealth liposomes
Stealth immunoliposomes
Brachial lymph nodes
Concentration (nmol/g)
5000
4000
3000
2000
1000
0
48
120
Time (h)
Cervical lymph nodes
Concentration (nmol/g)
3000
2500
2000
1500
1000
500
0
48
120
Time (h)
Mesenteric lymph nodes
Concentration (nmol/g)
50
40
30
20
10
0
48
120
Time (h)
Inguinal lymph nodes
Concentration (nmol/g)
100
75
50
25
0
48
120
Time (h)
Popliteal lymph nodes
Concentration (nmol/g)
150
100
50
0
48
120
Time (h)
Spleen
Concentration (nmol/g)
300
200
100
0
48
120
Time (h)

Figure 6

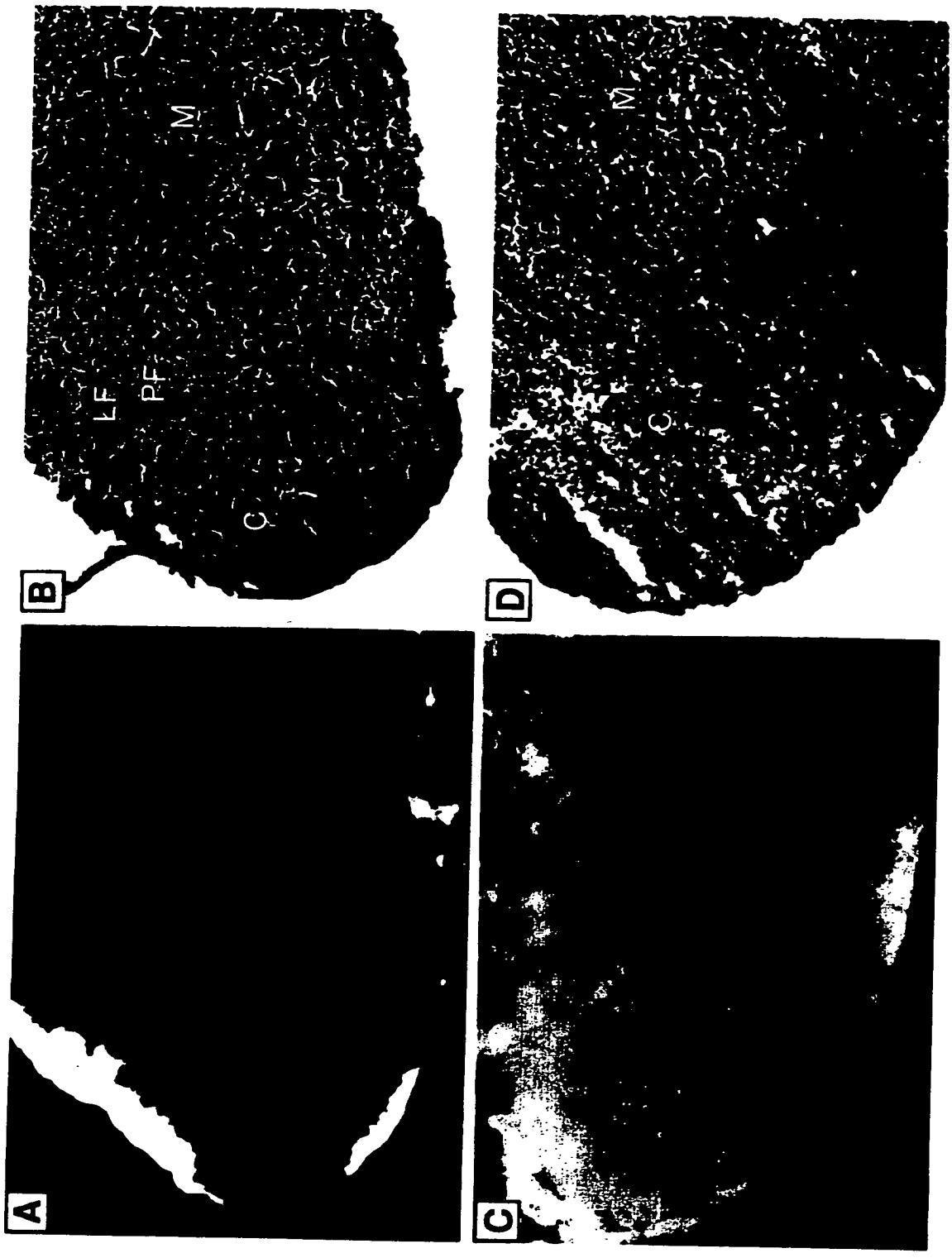

Figure 7

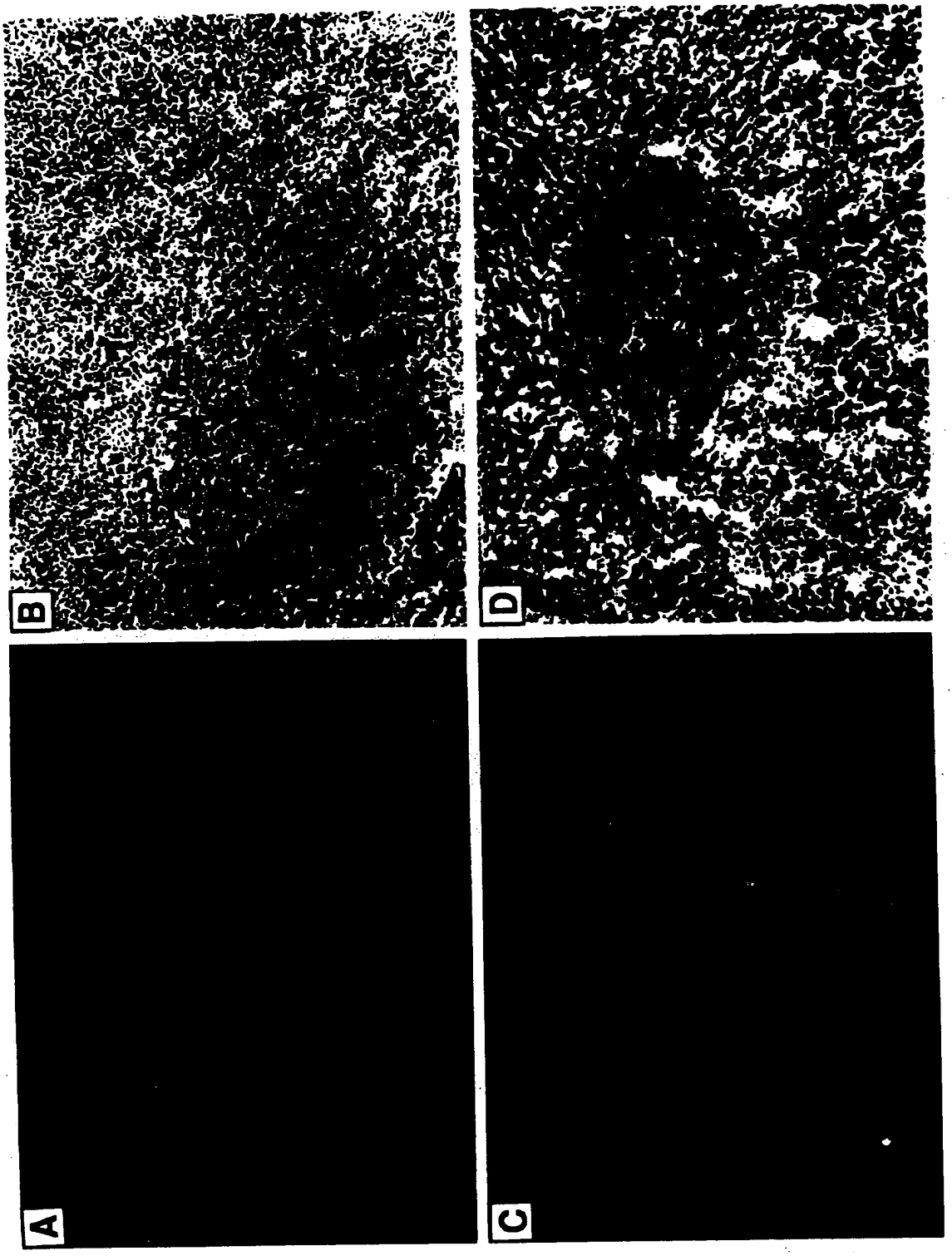

Figure 8

Cervical lymph nodes

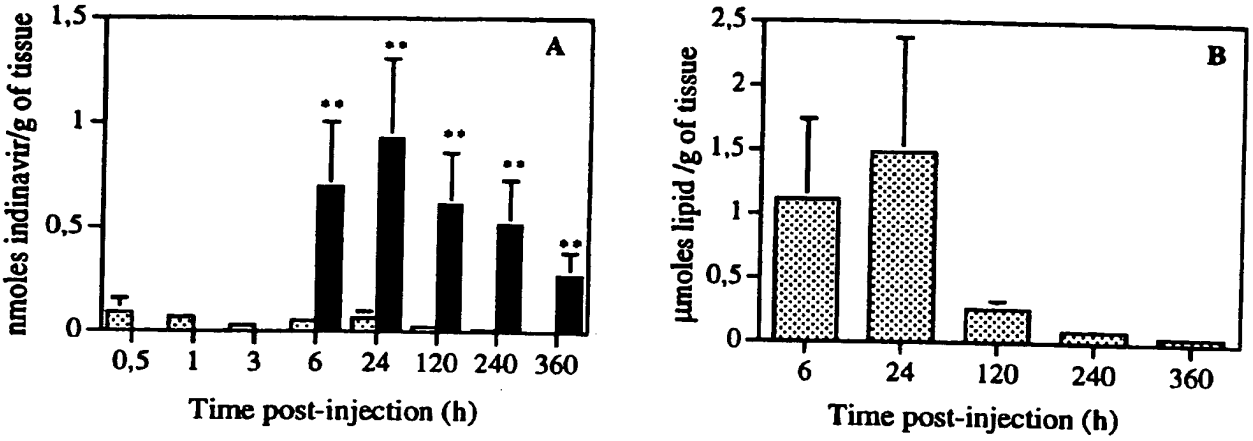

Brachial lymph nodes

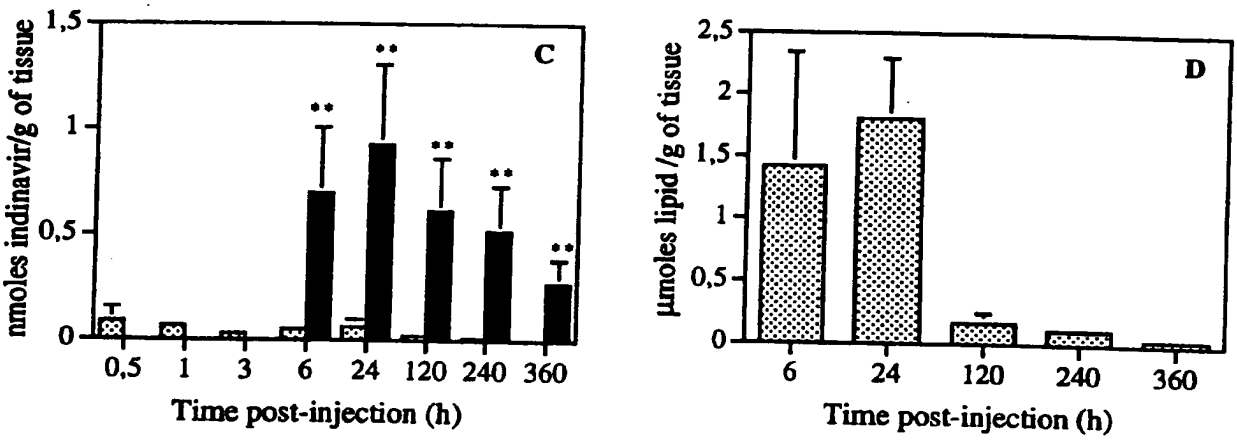

Mesenteric lymph nodes

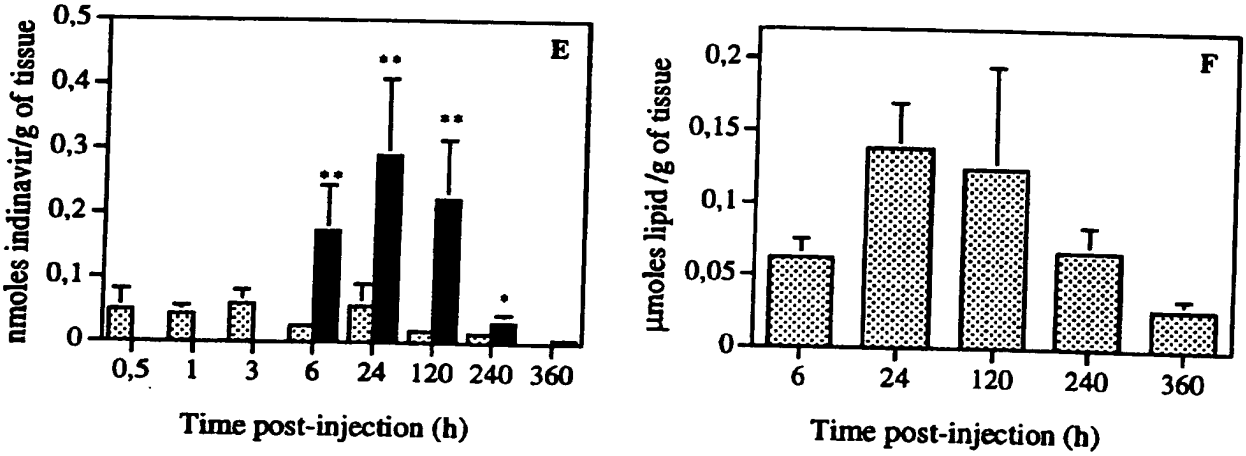

Figure 9

Inguinal lymph nodes

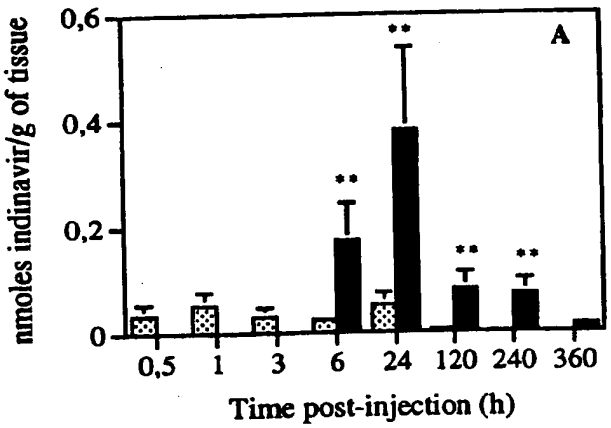

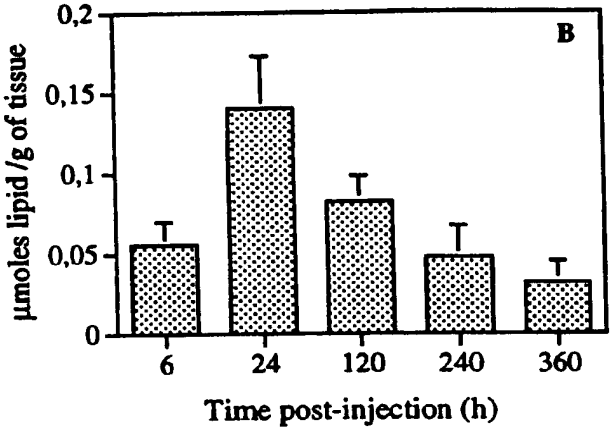

Popliteal lymph nodes

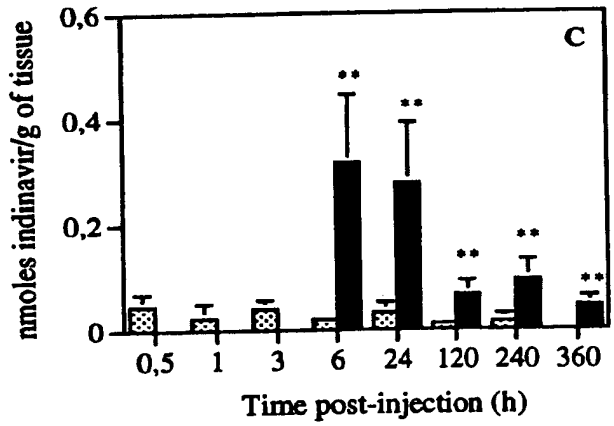

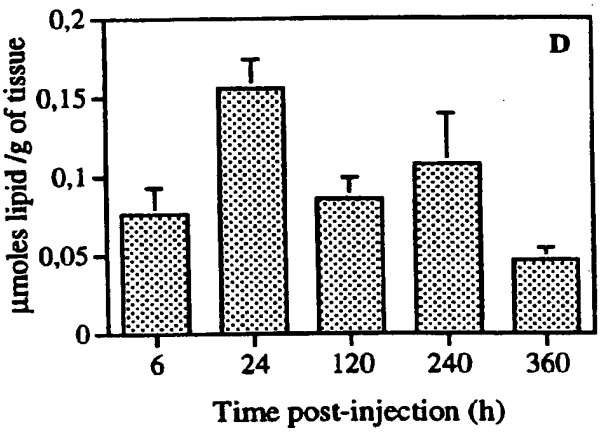

Spleen

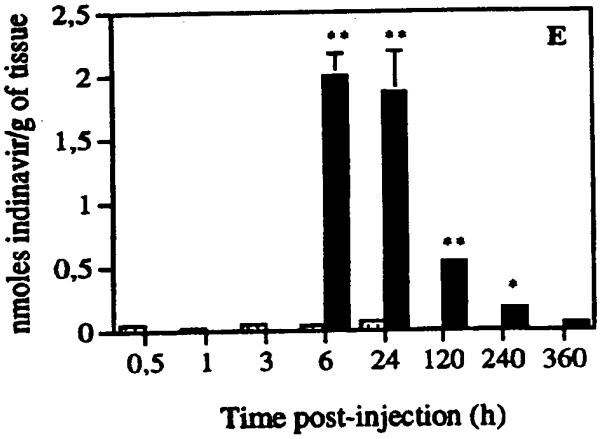

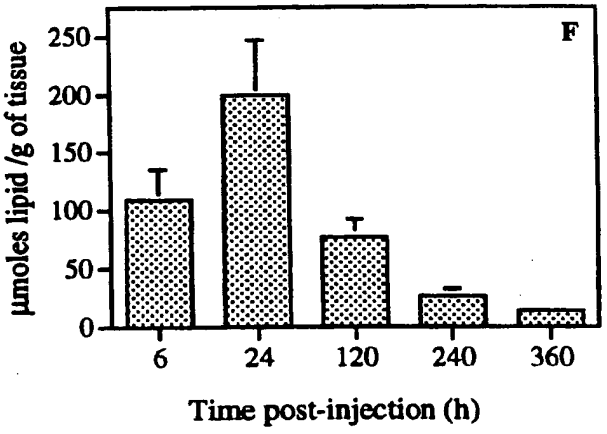

Figure 10

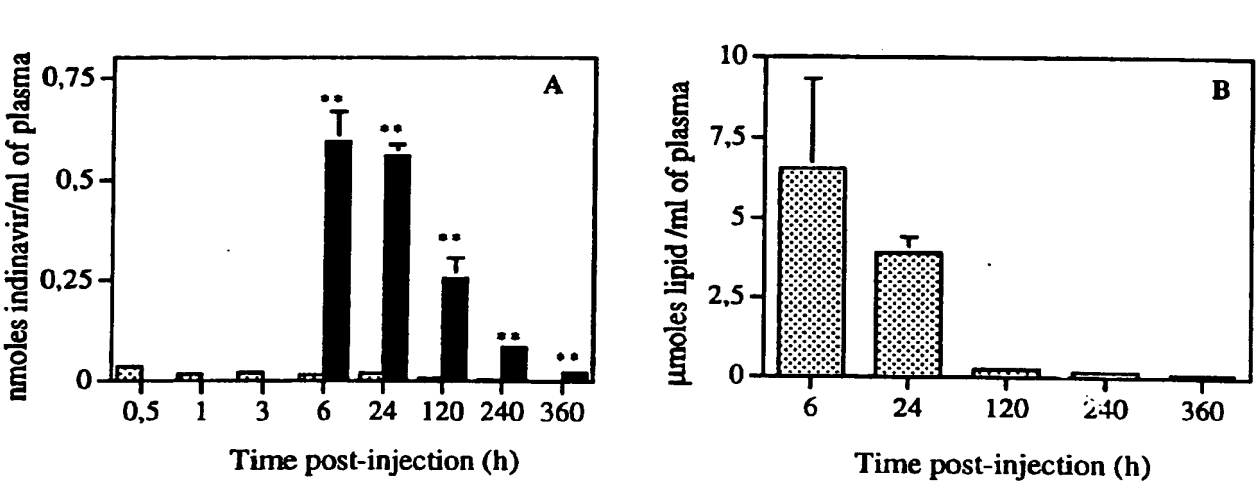
Plasma
nmoles indinavir/ml of plasma
0,75
0,5
0,25
0
A
0,5
1
3
6
24
120
240
360
Time post-injection (h)
µmoles lipid /ml of plasma
10
7,5
5
2,5
0
B
6
24
120
240
360
Time post-injection (h)

Figure 11

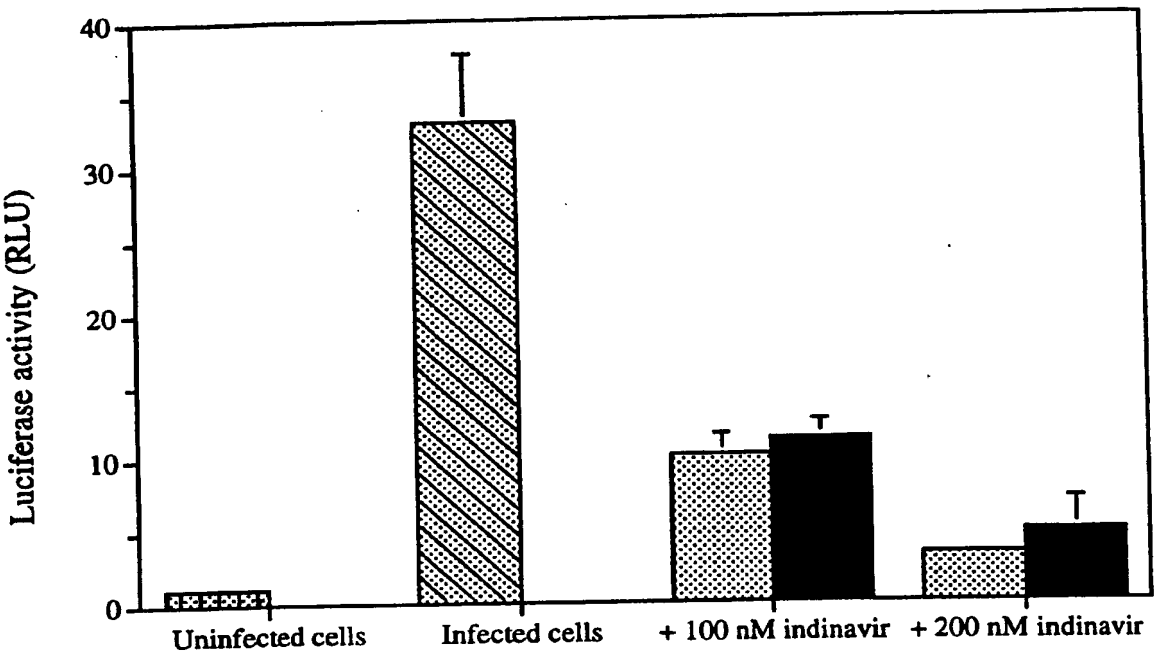
Luciferase activity (RLU)
40
30
20
10
0
Uninfected cells
Infected cells
+ 100 nM indinavir
+ 200 nM indinavir

Figure 12

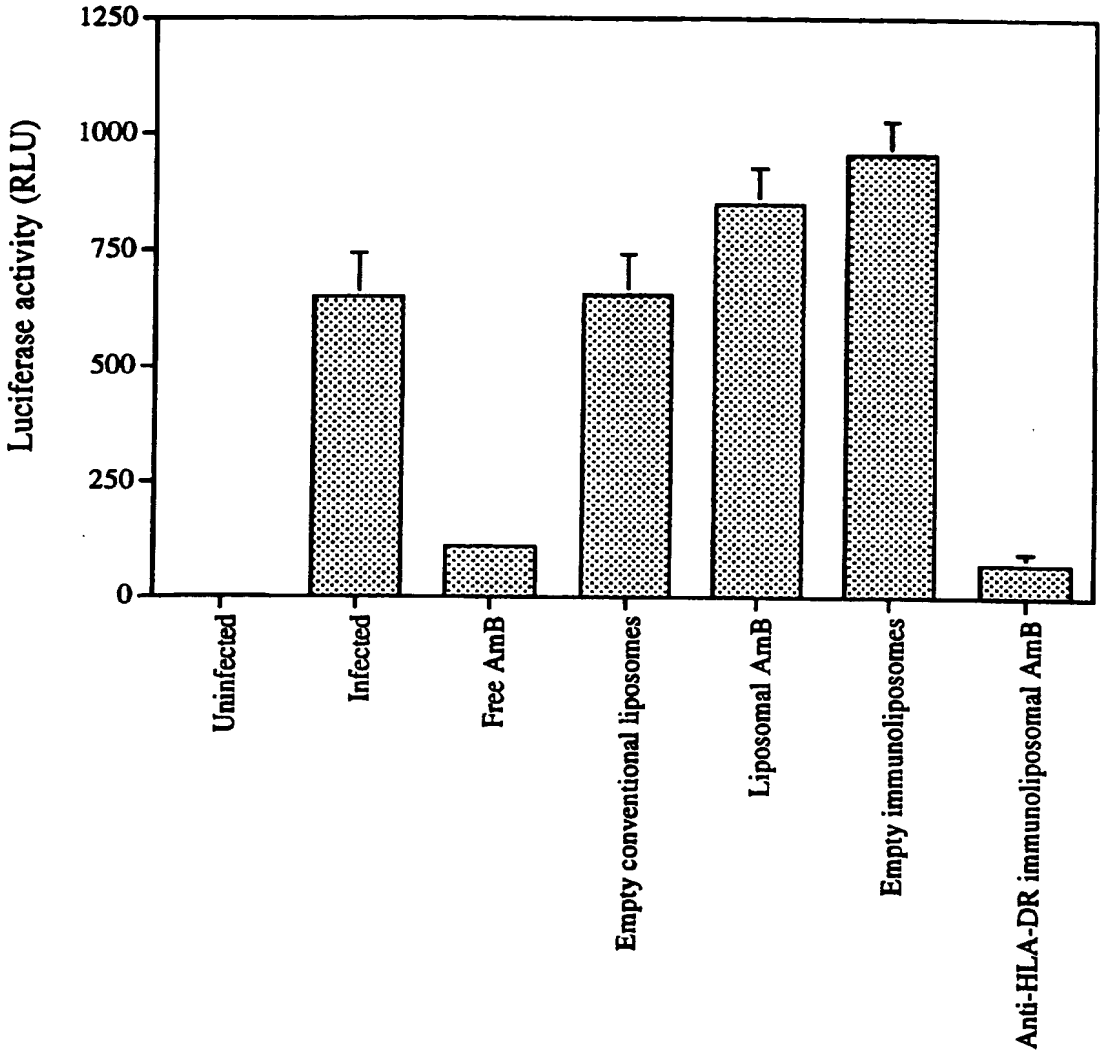
Luciferase activity (RLU)
1250
1000
750
500
250
0
Uninfected
Infected
Free AmB
Empty conventional liposomes
Liposomal AmB
Empty immunoliposomes
Anti-HLA-DR immunoliposomal AmB

Figure 13

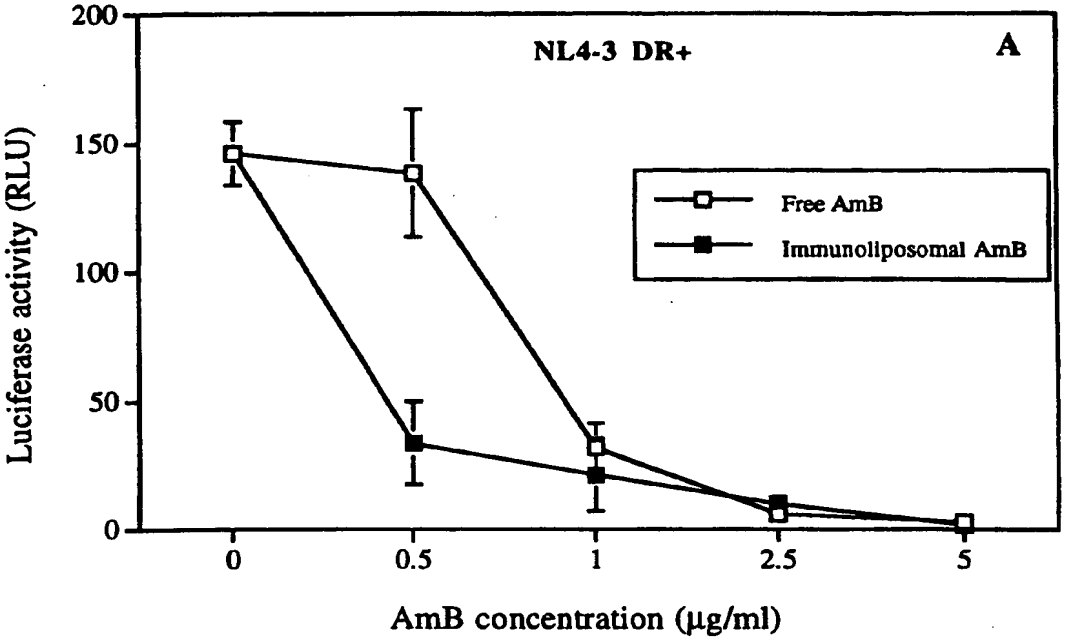
NL4-3 DR+
A
Luciferase activity (RLU)
200
150
100
50
0
Free AmB
Immunoliposomal AmB
0
0.5
1
2.5
5
AmB concentration (µg/ml)

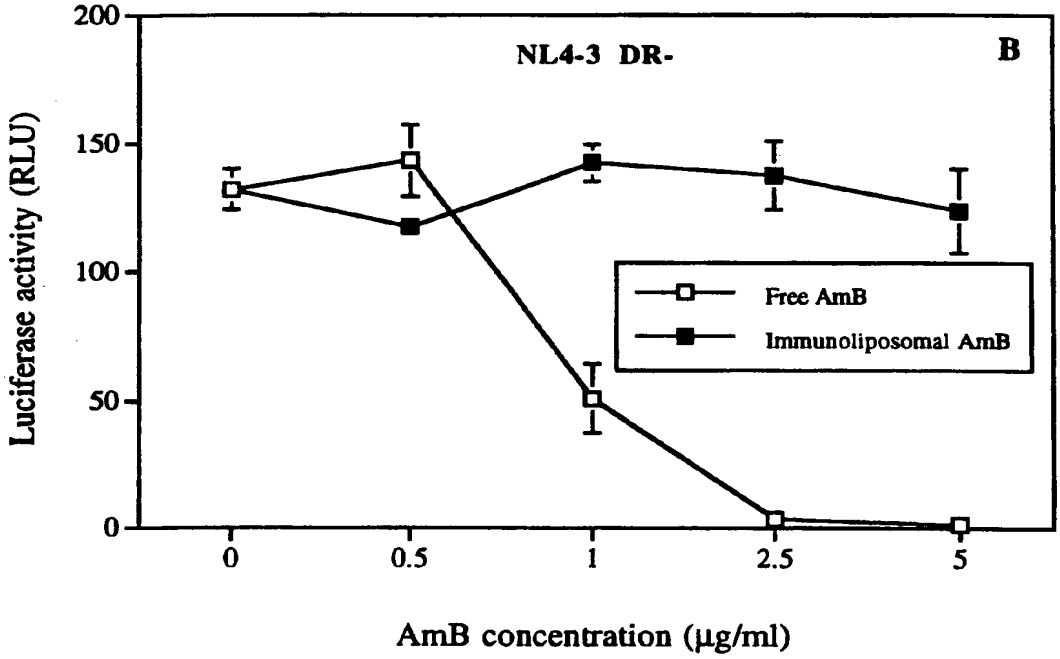
NL4-3 DR-
B
Luciferase activity (RLU)
200
150
100
50
0
Free AmB
Immunoliposomal AmB
0
0.5
1
2.5
5
AmB concentration (µg/ml)

Figure 14

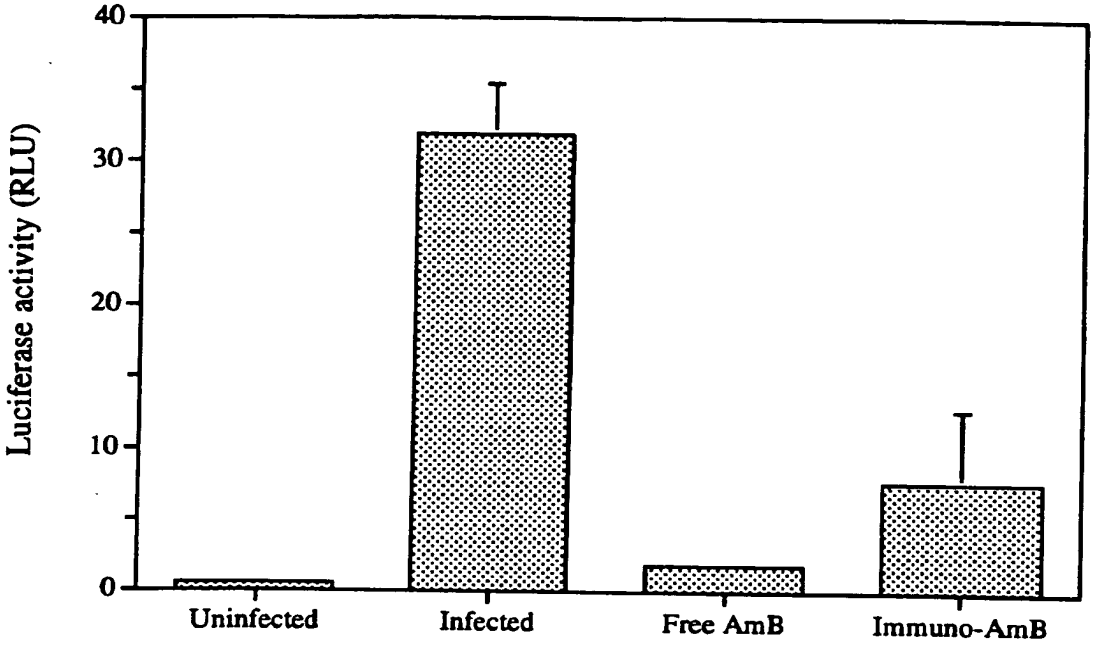
Luciferase activity (RLU)
40
30
20
10
0
Uninfected
Infected
Free AmB
Immuno-AmB

Figure 15

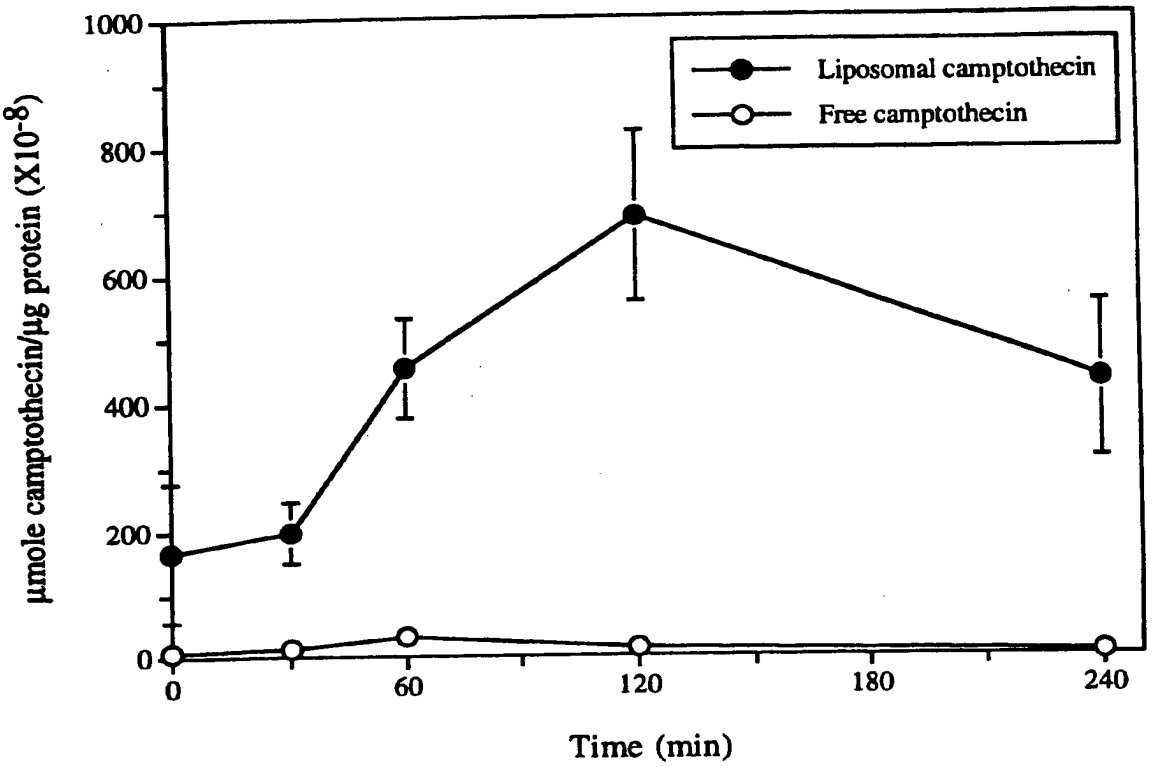
1000
800
600
400
200
0
µmole camptothecin/µg protein (X10-8)
Liposomal camptothecin
Free camptothecin
0
60
120
180
240
Time (min)

Figure 16

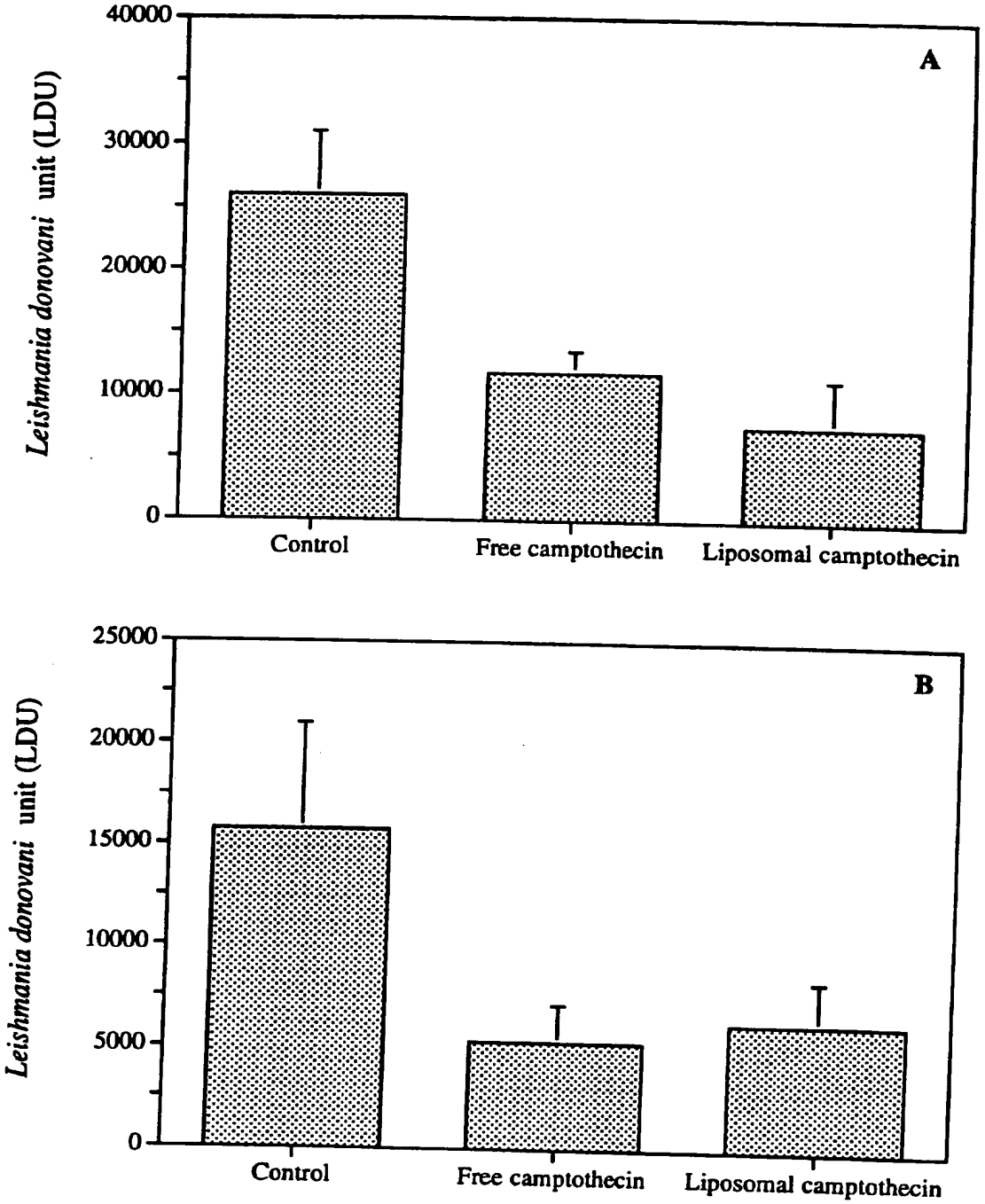
A
40000
30000
20000
10000
0
Leishmania donovani unit (LDU)
Control
Free camptothecin
Liposomal camptothecin
B
25000
20000
15000
10000
5000
0
Leishmania donovani unit (LDU)
Control
Free camptothecin
Liposomal camptothecin